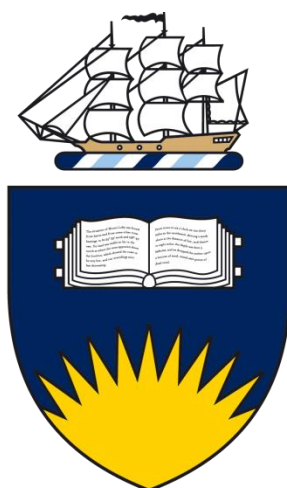


The Speciation of Gold in Mine Wastes and Natural Waters

A thesis submitted for fulfilment of the degree of
Doctor of Philosophy

Christine Ta

BTech (Forens&AnalytChem), BSc (Hons)



Flinders
UNIVERSITY

Faculty of Science and Engineering
School of Chemical and Physical Sciences

May 2013

6. Appendices

Appendix A

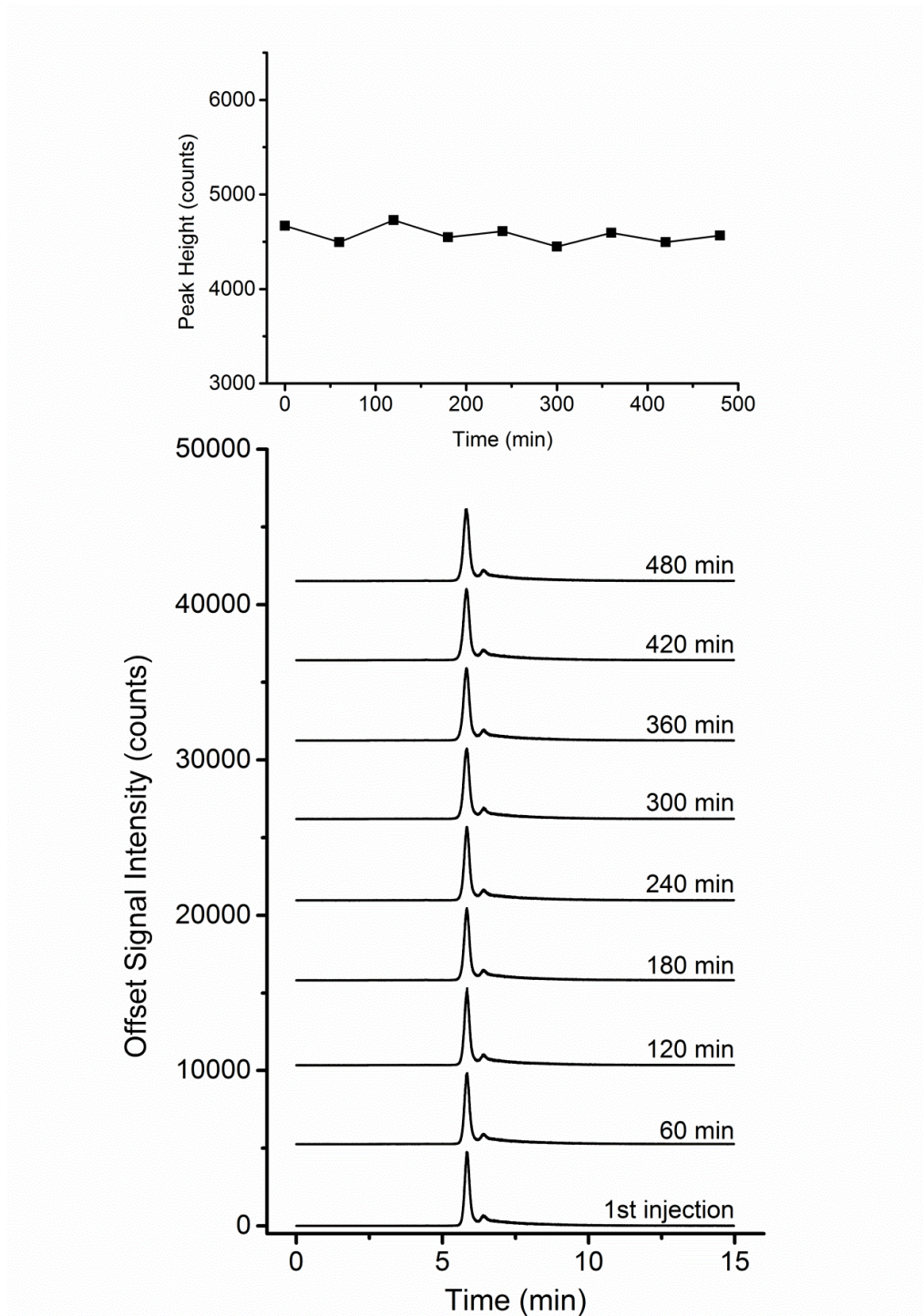


Figure 6-1 Effects of dilution and aging time on Au(I)-thiosulfate stability in water.

Chromatograms show injections of the standard spaced 60 minutes apart with an inserted plot of peak heights over time. The chromatograms are y-offset at intervals of ~5000 counts. Mobile phase: 6: 17.5 v/v isopropanol: acetonitrile, 1 mM TBAC, 5 mM $\text{NaH}_2\text{PO}_4/\text{Na}_2\text{HPO}_4$, pH 7.

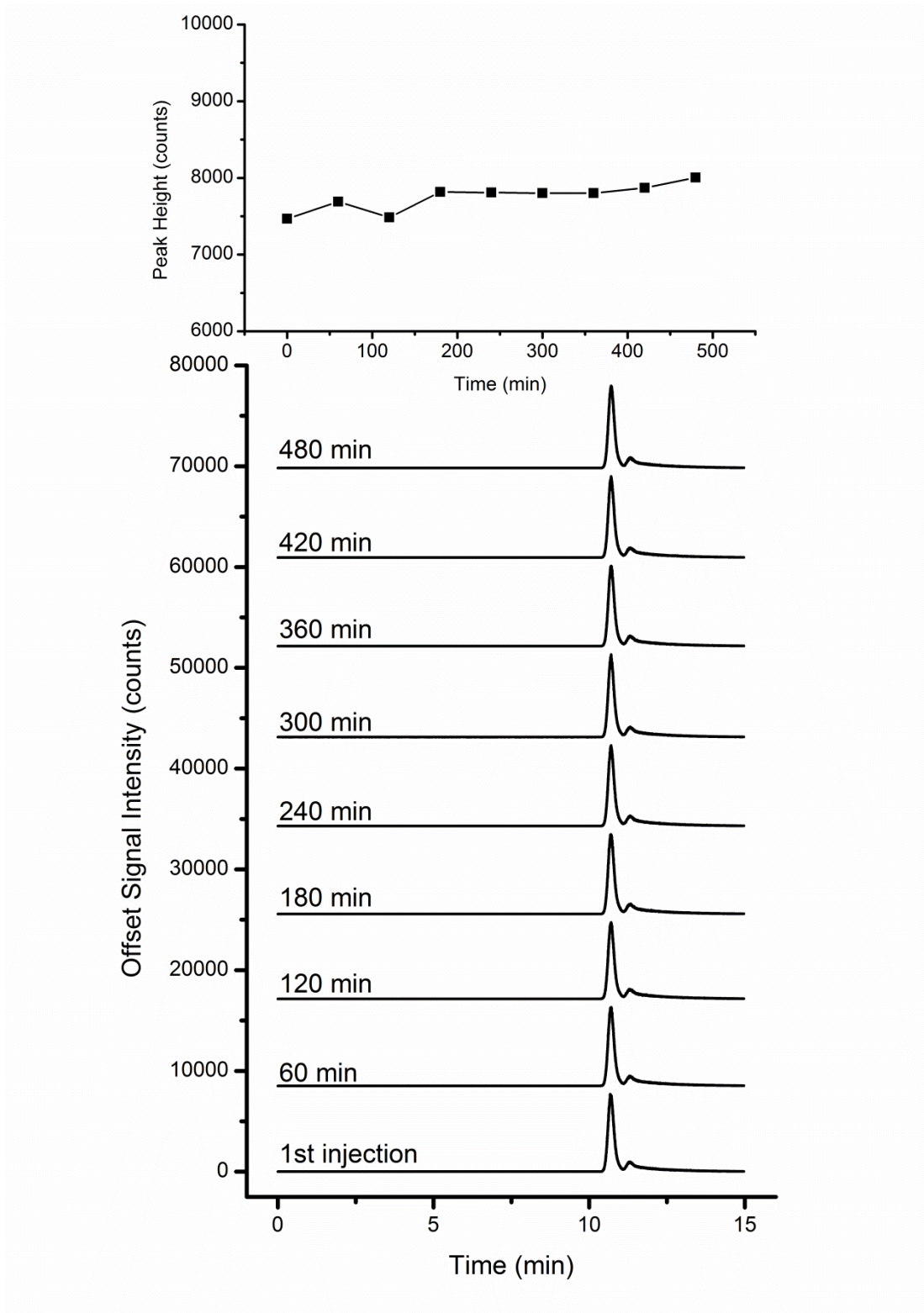


Figure 6-2 Effects of dilution and aging time on Au(I)-cyanide stability in water.

Chromatograms show injections of the standard spaced 60 minutes apart with an inserted plot of peak heights over time. The chromatograms are y-offset at intervals of ~8500 counts. Mobile phase: 6: 17.5 v/v isopropanol: acetonitrile, 1 mM TBAC, 5 mM $\text{NaH}_2\text{PO}_4/\text{Na}_2\text{HPO}_4$, pH 7.

Appendix B

The Challenger Gold mine samples that exhibited an additional peak around 1.3 minutes (Section 3.4.2) were reanalysed with the modified mobile phase to determine if this peak could be attributed to unretained components from the matrix. The retention time of the peak was unchanged with the new mobile phase, indicating that this peak was from the matrix, not a Au(III) complex.

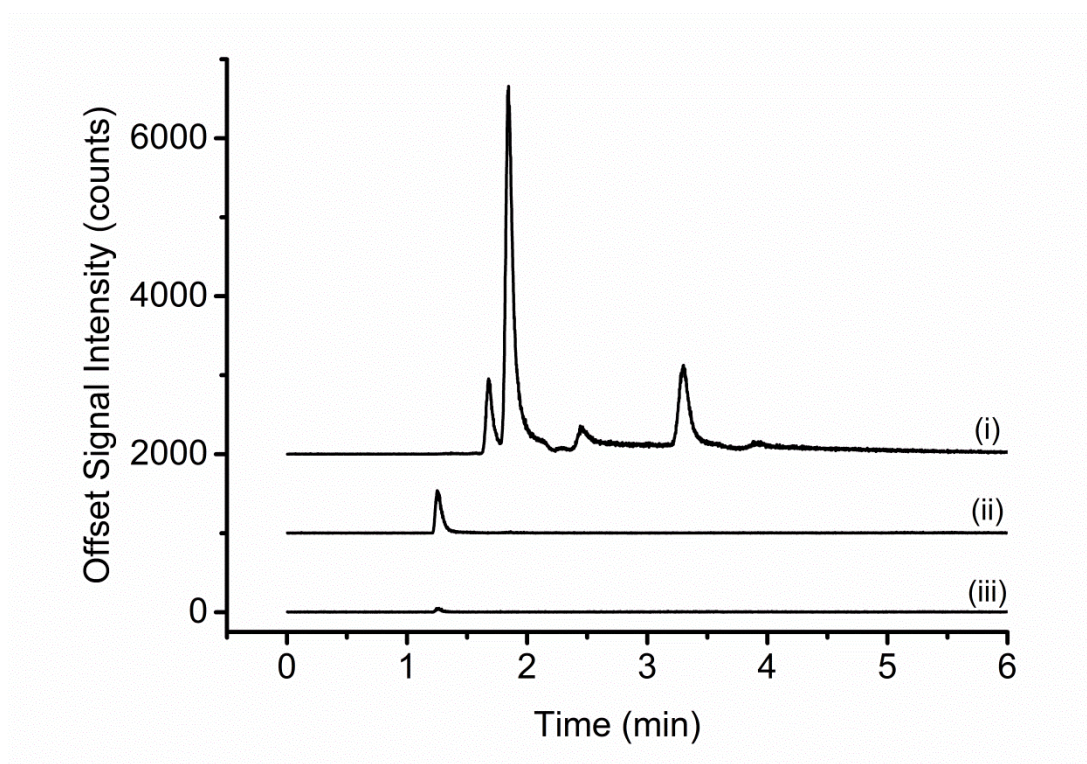


Figure 6-3 Effect of HDTMAOH on the unretained peak in Challenger mine wastes.

Chromatograms show (i) the shifted 100 mg L^{-1} of Au(III)-chloride and the unshifted matrix peaks at 1.3 minutes for the (ii) Challenger tailings and (iii) Challenger process water. Mobile phase: 6: 17.5 v/v isopropanol: acetonitrile, 1 mM ion-pairing agent (99:1 v/v TBAC:HDTMAOH), 5 mM $\text{NaH}_2\text{PO}_4/\text{Na}_2\text{HPO}_4$, pH 7.

Appendix C

X-ray Diffraction (XRD) Analysis

The natural samples listed in Table 4-2 were analysed with XRD to confirm that they were manganese minerals. All analyses were run by Dr. Barbara Etschmann from the South Australian Museum by room temperature powder XRD, using a Huber G760 100 mm image plate Guinier Camera with Co K α radiation ($\lambda = 1.78892 \text{ \AA}$). The samples were ground in acetone, spread uniformly on a MYLAR film and mounted on the sample oscillation unit for data collection.

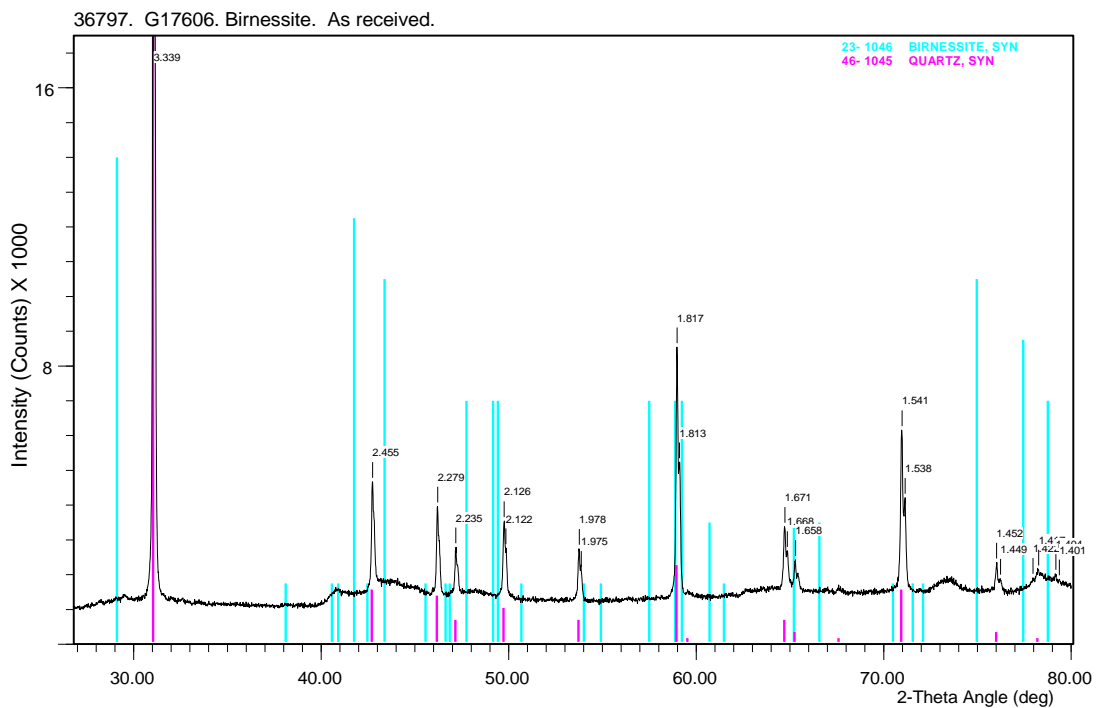


Figure 6-4 XRD pattern of G17606, birnessite.

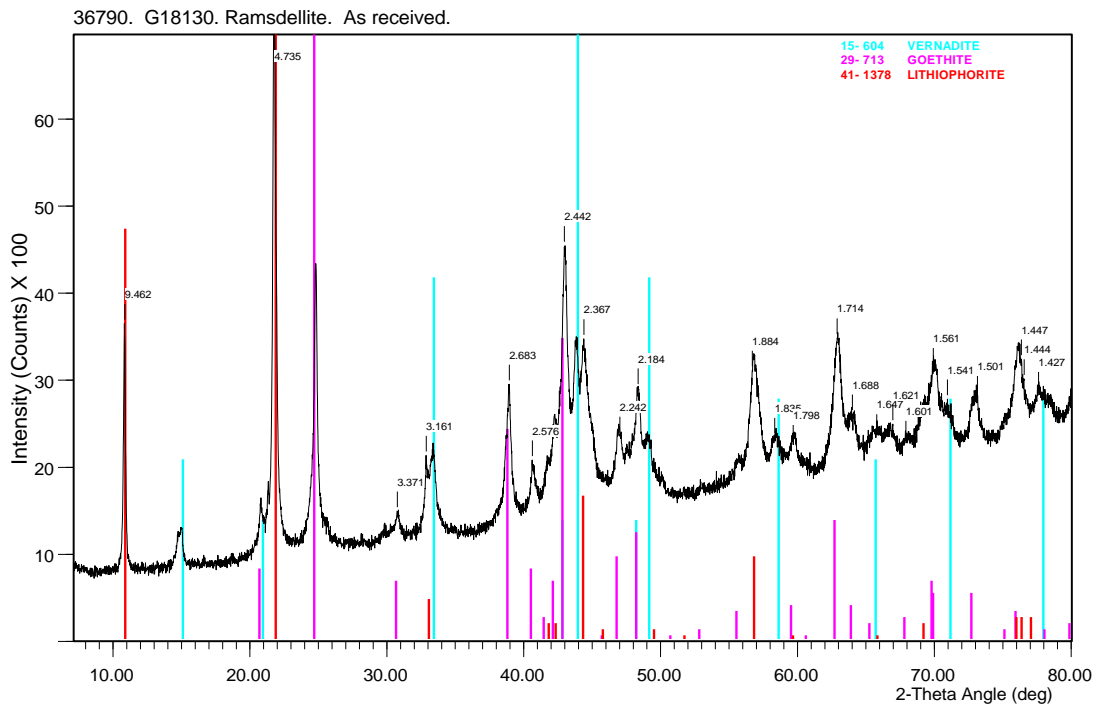


Figure 6-5 XRD pattern of G18130, lithiophorite/vernadite/goethite.

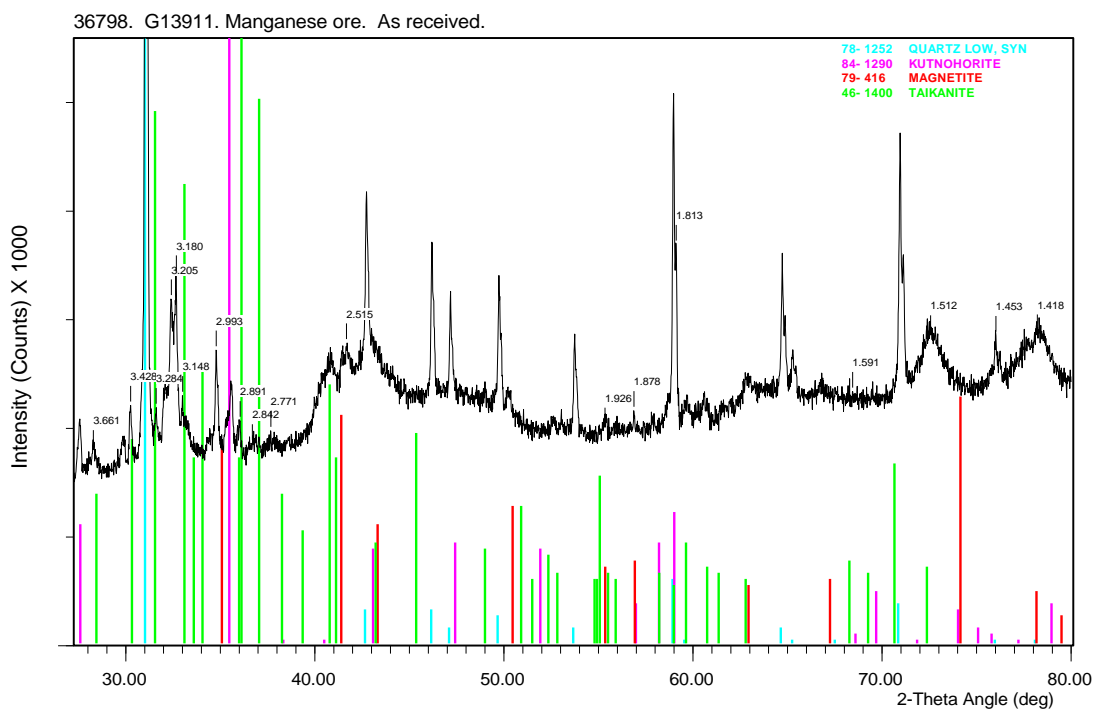


Figure 6-6 XRD pattern of G13911, kutnahorite.

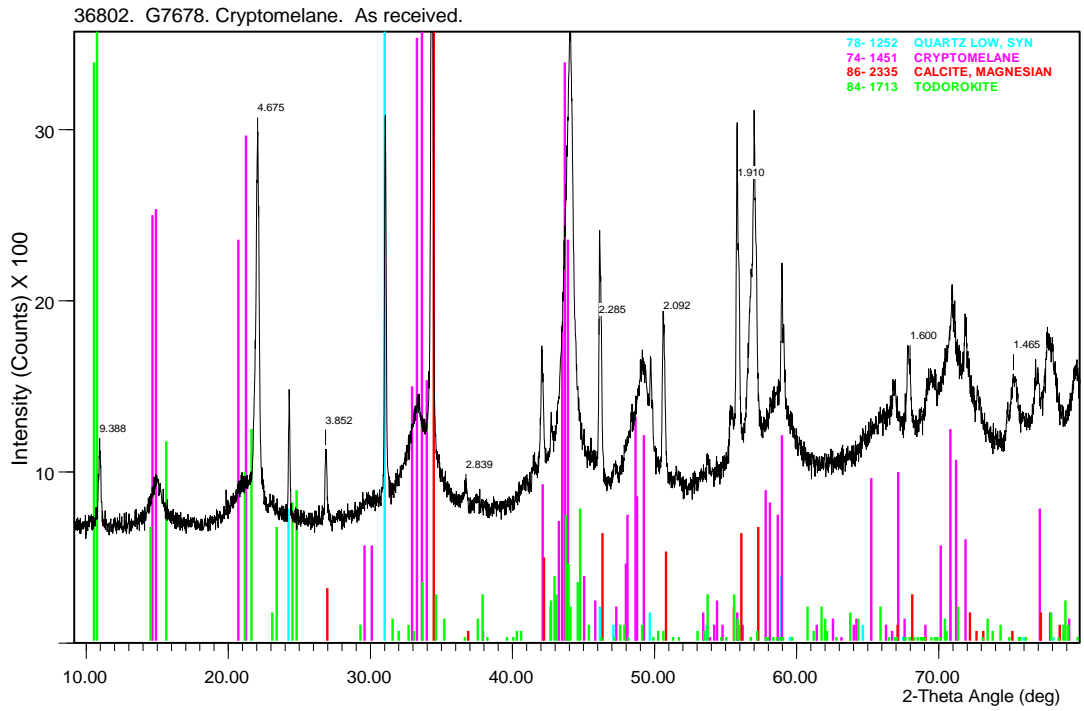


Figure 6-7 XRD pattern of G7678, Cryptomelane.

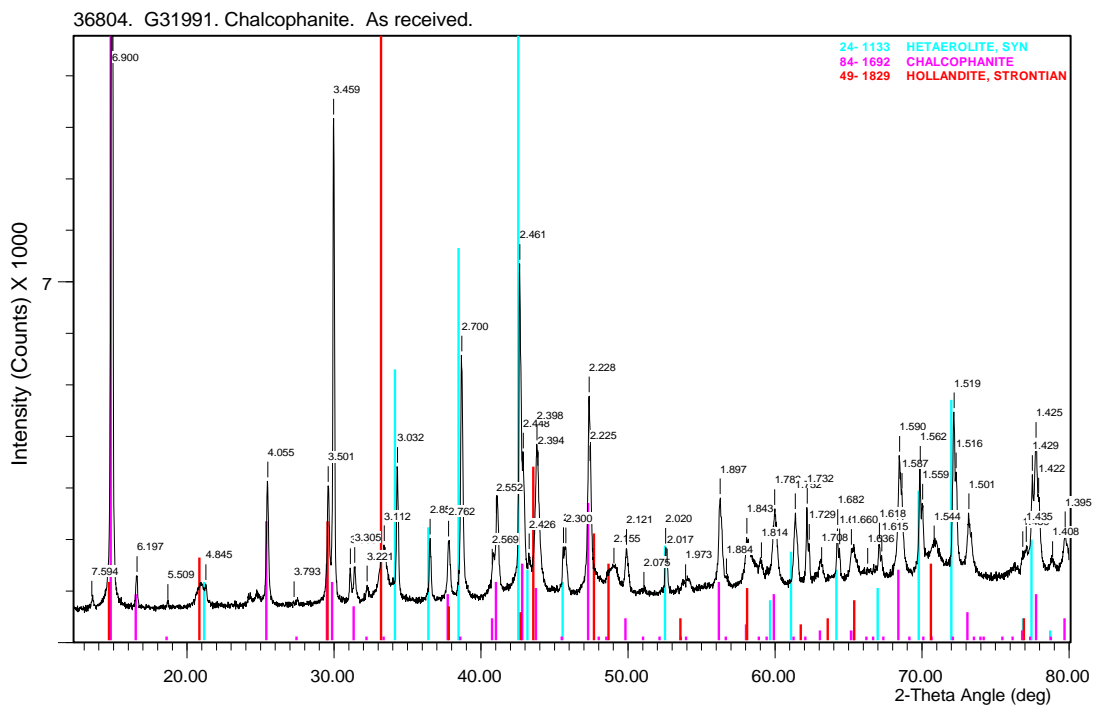


Figure 6-8 XRD pattern of G31991, hetaerolite/chalcophanite/hollandite.

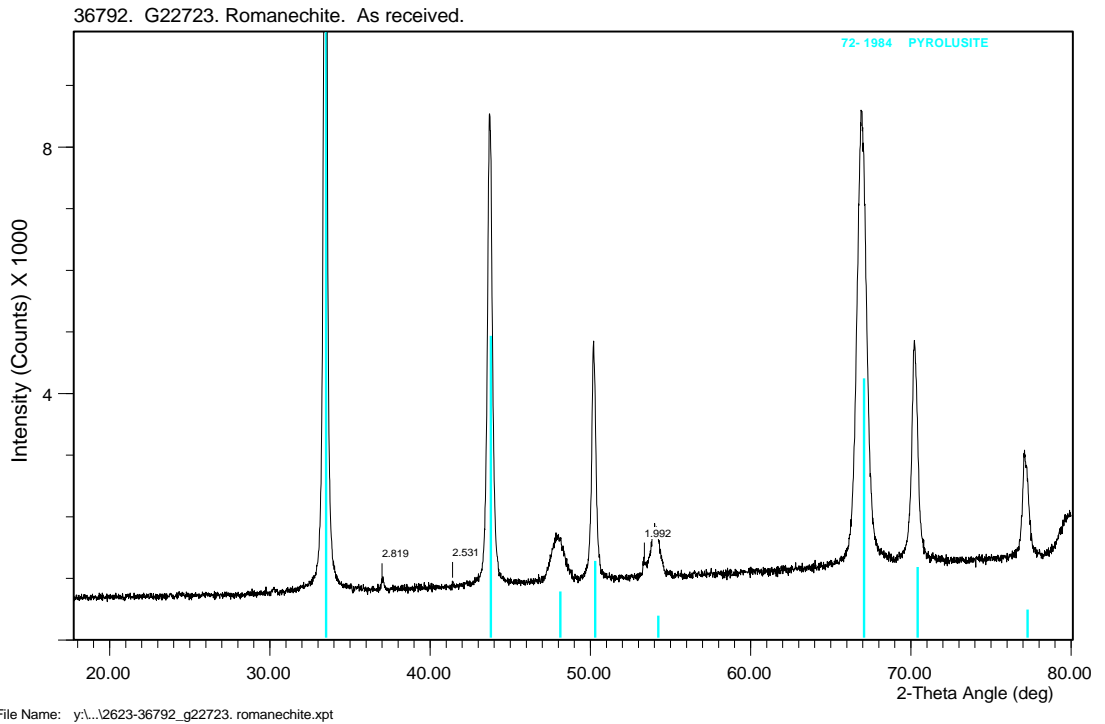


Figure 6-9 XRD of G30226, Pyrolusite.

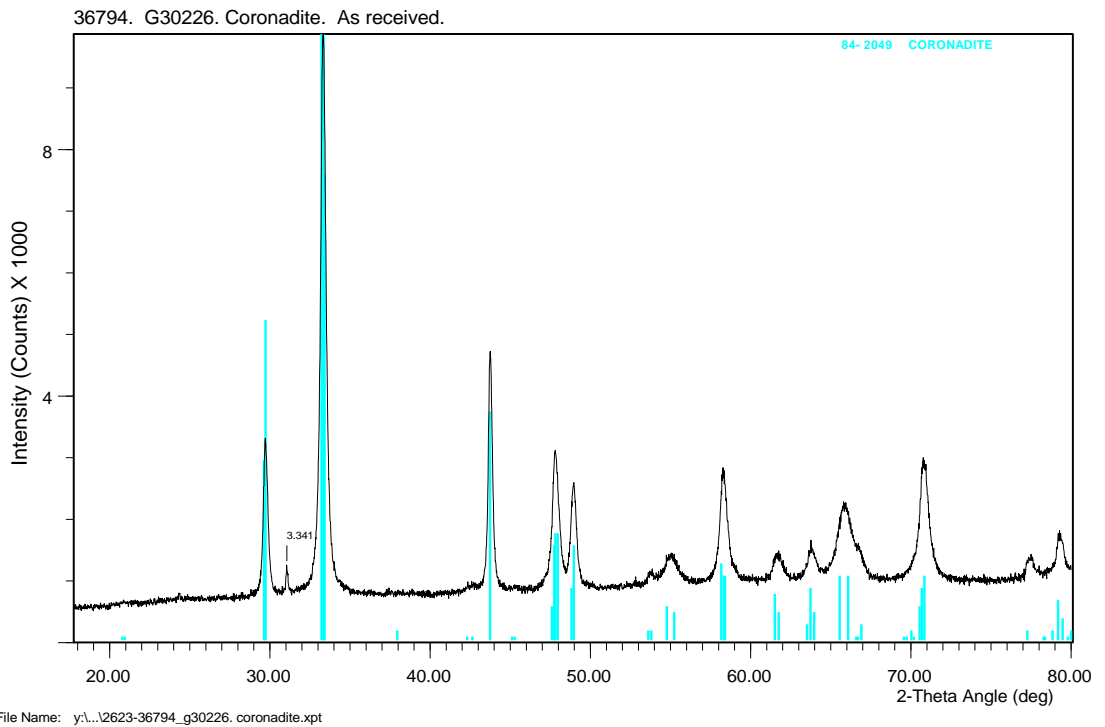


Figure 6-10 XRD of G30226, Coronadite.

Appendix D

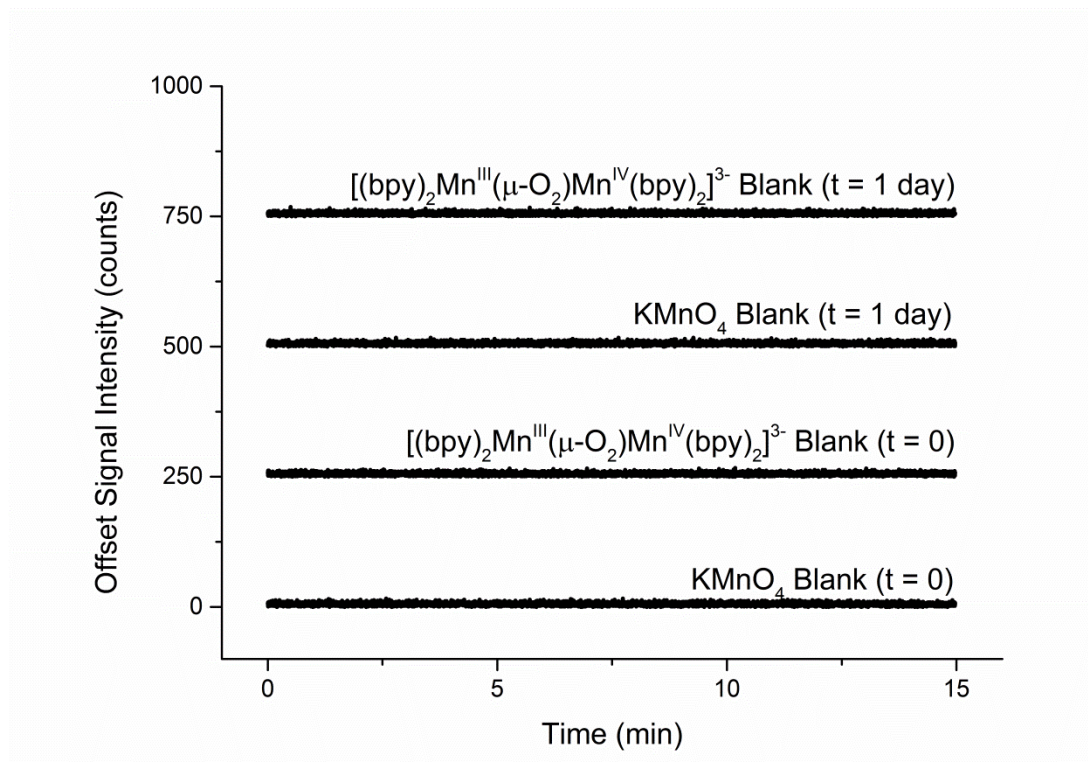


Figure 6-11 Effect of Cl^- ions on $[(bpy)_2Mn^{III}(\mu-O)_2Mn^{IV}(bpy)_2]^{3-}$ and permanganate solutions. Chromatograms of blank oxidation reactions (containing no Au); y-offset at intervals of ~250 counts. Solutions were diluted 20 times in water before analysis; Mobile phase: 6: 17.5 v/v isopropanol: acetonitrile, 1 mM TBAC, 5 mM NaH_2PO_4/Na_2HPO_4 , pH 7.